

# We are IntechOpen, the world's leading publisher of Open Access books Built by scientists, for scientists

6,900

Open access books available

185,000

International authors and editors

200M

Downloads

Our authors are among the

154

Countries delivered to

TOP 1%

most cited scientists

12.2%

Contributors from top 500 universities



WEB OF SCIENCE™

Selection of our books indexed in the Book Citation Index  
in Web of Science™ Core Collection (BKCI)

Interested in publishing with us?  
Contact [book.department@intechopen.com](mailto:book.department@intechopen.com)

Numbers displayed above are based on latest data collected.  
For more information visit [www.intechopen.com](http://www.intechopen.com)



---

# Fracture Theory Under Freeze-Thaw Cycles and Freeze-Thaw Resistance of Alkali-Slag Concrete

---

Qixuan Li

Additional information is available at the end of the chapter

<http://dx.doi.org/10.5772/63810>

---

## Abstract

Despite the widespread research on alkali-activated concrete, its fracture properties under freeze-thaws are rarely studied; the response surface methodology (RSM) theory has not been put forward; and unstable fracture toughness,  $K_{IC}^S$ , influenced by freeze-thaws and slag content has not been researched. The purpose of this article is to investigate the calculation method of alkali-slag concrete (ASC) fracture parameters and provide theoretical support for RSM model of ASC prepared with  $\text{Na}_2\text{SiO}_3$  and NaOH composite activator. The influence law of freeze-thaw and slag content on unstable fracture toughness,  $K_{IC}^S$ , is put forward. Results show that after crack mouth opening displacement (CMOD) is measured, other fracture parameters including concrete effective fracture length; crack tip opening displacement (CTOD); and stress intensity factors  $K_{IC}^C$ ,  $K_{IC}^C$ , and  $K_{IC}^S$  from closure stress  $\sigma(w)$  can be obtained according to double- $K$  fracture criterion and DL/T 5332-2005 "Hydraulic concrete fracture test procedures". RSM principles and advantages, its optimization content and procedure, the data processing software Design-Expert and verification analysis procedure of RSM model are put forward. Since the ASC structure is compact, characterized for water and air penetration resistance, its antifreezing characteristic is desirable.

**Keywords:** alkali-slag concrete, fracture parameter, response surface theory, unstable fracture toughness, composite activator

---

## 1. Introduction

It has been nearly 200 years since the advent of Portland cement in 1824. Then there were mortar, concrete and reinforced concrete generated from it. Concrete has become the most widely and

---

largely used construction material. Construction of highways, bridges, ports, oil platforms, airports, dams, tunnels; underground constructions; and construction above and under sea level are all inseparable from concrete. Today, with the continuous progress of human demand and technology, research on concrete materials and structures is constantly moving toward depth and breadth. High performance and new special concrete is more and more widely used in projects, the construction technology is also maturing day by day.

With social progress and the advent of low-carbon economy, environmental protection and sustainable development attract more and more attention around the world. However, cement production causes serious pollution and consumes a large amount of energy and nonrenewable resources such as coal, using large amount of limestone, iron ore, clay, etc. The traditional production process emits large amount of dust, and also exhausts huge amount of  $\text{CO}_2$ ,  $\text{SO}_2$ ,  $\text{NO}_x$  and other emissions. It is calculated that 1 t of cement clinker's atmospheric emissions will be 1 t of  $\text{CO}_2$ , 0.86 kg of  $\text{SO}_2$ , 1.75 kg of  $\text{NO}_x$  and 130 kg of dust. Cement production will continue to see a significant increase from the existing level, which will cause serious burden on the environment.

Production of new green and high performance concrete should make full use of industrial waste, such as slag, fly ash, limestone, gangue, etc., with no or little use of cement clinker. Minimizing clinker production reduces the environmental impact, and making new "cement" through technical means results in green cementitious materials.

Most of the world is in cold region, where winter temperature is below  $-5^\circ\text{C}$  and concrete damage in those areas is the most relevant to freezing and thawing. Hypothermia is very unfavorable for concrete; the low temperature and freeze-thaw cycles usually lead to concrete deterioration in airports, highways, bridges, hydraulic structures, etc. Freeze-thaw damage is a persistent historic problem, receiving widespread attention from academia and engineering field. Internationally renowned concrete expert Sun proved in 1999 that the concrete damage process is accelerated and the extent of damage increased under the simultaneous action of load and freeze-thaw cycles [1]. Therefore, freezing is an important factor affecting the durability of concrete structures. Where there are alternating positive and negative temperatures, there exists concrete freeze-thaw damage.

During freeze-thaw process, there are heaving pressure cycles inside the concrete material, producing freeze-thaw internal stress. The structural organization will appear in irreversible microscopic changes such as microcrack formation, expansion, empty initiation and crystal dislocations. Internal concrete defects will gradually expand and accumulate, causing deterioration of material macroscopic mechanical properties, and resulting in damage. Damage caused by freeze-thaw stress gradually accumulates with freeze-thaw cycles, resulting in deterioration and even damage in concrete, which can be explained with percolation theory and damage theory, namely no damage  $\rightarrow$  damage (formation of microcracks)  $\rightarrow$  macrocracks  $\rightarrow$  damage.

Thus, concrete freeze-thaw damage mechanism mainly lies in various microcracks, defects formation and expansion under external freeze-thaw cycles, resulting in damage and failure. Concrete freeze-thaw damage process indicates its complicated constitutive behavior, and it

would be difficult to achieve the desired results if only describing with classical elastic or plastic mechanics. In order to fully reflect mechanical behavior of concrete structures under external factors, concrete body must be treated as deformable solid containing microcracks, other defects and even macroscopic cracks, and studied with fracture mechanics and damage mechanics.

There are many studies about alkali-activated concrete these years including application in railway sleepers [2], characteristics after exposure to high temperature [3], mixed fine aggregates [4], static and dynamic performances [5], mechanical properties [6], durability [7], eco-efficiency [8] and heat resistance characteristics [9]. Ravikumar [10] and Neithalath [11] successively published papers about chloride ion transport and electrical impedance of alkali-activated slag concrete. Qixuan [12] proposed the RSM model for ASC fracture property prediction. However, the RSM theory has not been clarified and systematically studied. Provis [13] summarized the progress in understanding alkali-activated materials since 2011, which is of great value. Kovtun [14] studied the chemical acceleration of blastfurnace slag activated by sodium carbonate. Ma [15] corrected one misunderstanding in the shrinkage of alkali-activated fly ash, and is beneficial for future researchers. Ke [16] implemented calcined layered double hydroxides into the controlling of sodium carbonate-activated slag cements.

As can be seen, fruitful research results have been achieved in concrete deterioration and damage, but most of them focus on properties under load conditions at room temperature, ignoring environmental impact on concrete mechanical properties. There is little research on concrete fracture properties under freeze-thaw cycles, even less analyzing concrete fracture behavior and fracture characteristics after freeze-thaw cycles. Since fracture toughness is an important basis for the analysis of concrete crack propagation stability, it is extremely urgent and necessary studying concrete fracture properties under freeze-thaw cycles.

Through calculating, calculation method of ASC fracture parameters such as critical effective fracture length  $a_c$ , stress intensity factor  $K_{IC}^C$  caused by closure stress, initiation toughness  $K_{IC}^Q$  and unstable fracture toughness  $K_{IC}^S$  are investigated. The response surface methodology theory is systematically put forward, including RSM principles and advantages, optimization content and procedure, data processing software Design-Expert and verification of RSM model. Influence law of freeze-thaw on  $K_{IC}^S$  under different slag content is studied.

## 2. Test materials and methods

### 2.1. Raw materials and preparation

ASC material consists of a quaternary system (slag, activator, sand, stone), and the correct choice of raw material is especially important. Through investigation and analysis, this chapter ultimately determines the test raw materials as follows:

### (1) Activator

Type and dosage of activator have a great impact on ASC performance. Currently, there are  $\text{Na}_2\text{SiO}_3$  or  $\text{K}_2\text{SiO}_3$  water glass solution and  $\text{NaOH}$  or  $\text{KOH}$  solution, and alkali metal carbonates and alkaline earth metal chlorides, among which water glass is more widely used and has better properties.

In this study, the activator is composed of  $\text{Na}_2\text{SiO}_3$  sodium silicate (27.21%  $\text{SiO}_2$ , 8.14%  $\text{Na}_2\text{O}$ ,  $M_s = 3.1$ ) and  $\text{NaOH}$  complex solution, which density was  $1.43 \text{ g/cm}^3$ .

### (2) Blast furnace slag powder

Blast furnace slag powder is a pig iron smelting slag discharged from the blast furnace. From the aspect of chemical composition, blast furnace slag belongs to silicate material, whose chemical compositions are mainly  $\text{CaO}$ ,  $\text{Al}_2\text{O}_3$ ,  $\text{SiO}_2$ , and the content is generally above 90%. In addition, there are  $\text{MgO}$ ,  $\text{MnO}$ ,  $\text{Fe}_2\text{O}_3$ ,  $\text{CaS}$ ,  $\text{FeS}$  and  $\text{TiO}_2$  chemical compositions.

The metallurgy blast furnace slag powder used in this study has the specific surface area of  $410 \text{ m}^2/\text{kg}$  and density of  $2.86 \text{ g/cm}^3$ . The main chemical composition of slag powder is shown in **Table 1**.

CaO	SiO <sub>2</sub>	Al <sub>2</sub> O <sub>3</sub>	MgO	MnO	Fe <sub>2</sub> O <sub>3</sub>	TiO <sub>2</sub>	Loss
38.95	33.91	10.71	9.41	0.31	3.28	3.43	1.27

**Table 1.** Chemical compositions of slag/w%.

According to GB/T 18046-2000 "Ground granulated blast furnace slag used for cement and concrete" [17], GB/T 18736-2002 "Mineral admixtures for high strength and high performance concrete" [18] and GB/T 12957/2005 "Test method for activity of industrial waste slag used as addition to cement" [19], 7 and 28 days activity indexes of the slag are 96.2% and 105.7%, which are high.

### (3) Fine aggregate

Fine aggregate should be hard, durable, clean, with smooth grain shape, good gradation and suitable fineness modulus, and the impurity should be less than a predetermined value. Besides, the natural river sand should be preferred, because it is generally hard, with good grain shape and low clay content, which is beneficial to the fresh concrete workability and hardened concrete performance. When using artificial sand, it should paid attention that the content of coarse particles and small particles are not too high. Zone II river sand should be preferred in concrete preparation.

The role of fine aggregate in the ASC is similar to forkability and strengt with filling effect on the one hand, while being the bond between coarse aggregate and cementitious materials on the other hand. This chapter uses natural river sand with fineness modulus of 2.86, densi-

ty of 2.63 g/cm<sup>3</sup>, bulk density of 1.50 g/cm<sup>3</sup> and 0.5% clay content. Gradation screening testing results are shown in **Table 2**.

Particle size/mm		Accumulated sieve (by mass)/%				
		Mesh size (square hole sieve)/mm				
		2.36	4.75	9.50	19.0	37.5
Screening results	5–10	100	68	1	–	–
	10–20	100	97.2	81.5	18	–
	20–40	–	–	–	100	0
After screening	5–40	–	95.86	84.6	65.4	0

**Table 2.** Fine aggregates screening test results.

#### (4) Coarse aggregate

Coarse aggregates commonly used in concrete are gravel and pebbles. The coarse aggregate should be hard, durable, clean and has a certain gradation. The main technical requirements are as follows:

1. Varieties: coarse aggregate should be hard texture unweathered rock, such as basalt, limestone, granite and diabase. The more dense is the rock, the lower is the water absorption, the smaller is the crushing index and the better are the mechanical properties.
2. Grain shape: rough gravel with angular is generally used; gravel grain shape produced by hammer crusher is good, which has good mechanical properties, and can bond relatively more firm with cement. Flakiness particle content should not be over 5%, and the clay content should not exceed 1.0%.
3. Grading: to obtain dense concrete, coarse aggregate should have a good grading. With good grading, the porosity will be small, less cement will be needed to achieve the same mobility and concrete shrinkage deformation will be small, forming good volume stability to enhance strength and durability.

This chapter uses limestone gravel (45% 5–20 mm, 55% 20–40 mm) with density of 2.76 g/cm<sup>3</sup> and bulk density 1.69 g/cm<sup>3</sup>.

#### 2.2. Workability and strength test

Test workability according to GB/T 50080-2002 “Standard for test method of performance on ordinary fresh concrete” [20]. The measuring method is as follows: Add the concrete mix according to the provided method into the standard tapered slump cone (bottomless). After the cone is filled elaborately, lift the cartridge straight up. The mixture will appear slump

because of its own weight. Measure the size of the downward slump (mm), which is slump as liquidity indicator, as shown in **Figure 1**.



**Figure 1.** Determination of concrete mixture slump.

When measuring the fresh concrete slump, visually evaluate the following properties at the same time:

1. Cohesiveness: observe the mutual cohesion situation of the components. Use a tamper to tap on the concrete cone side already slumped, if the cone gradually sinks after tapping, the mixture cohesiveness is favorable; on the other hand, if the cone suddenly collapses, partially crack or the stones segregate, it means that its cohesiveness is bad.
2. Water retention: According to the condition of water saturating out of the mixture, there are three degrees as “a lot”, “small” and “no”.

“A lot” means that there is much water separating out of the bottom after pulling up the slump cone; “small” indicates that a small amount of water comes from the cone after it is pulled up; and “no” means that no water penetrates from the cone even it is pulled up.



**Figure 2.** Wt60 t Universal Bending Test Machine and 200 t Compression Testing Machine.

According to GB/T 50081-2002 “Standard for test method of mechanical properties on ordinary concrete” [21], strength tests are carried out using wt60 and 200 t Universal Testing Machine (as shown in **Figure 2**). Test the specimen flexural and compressive strength after 7 and 28 days of curing.

### 3. ASC fracture properties under freeze-thaw cycles

#### 3.1. Fracture toughness parameter calculation method

Crack mouth opening displacement (CMOD) was measured directly using clip-on extensometer. The extensometer was connected to computer automatic acquisition system, through which loads could be obtained [22]—crack mouth opening displacement curve under loads, which is P-CMOD curve to get  $CMOD_C$ . At the same time, the test can also directly measure ASC load-displacement curve that is P-V curve, and take the load when the specimen fractures at ultimate load  $P_{max}$ . After  $P_{max}$  and  $CMOD_C$  are set, concrete effective fracture length; crack tip opening displacement CTOD; and stress intensity factors  $K_{IC}^C$ ,  $K_{IC}^Q$  and  $K_{IC}^S$  from closure stress  $\sigma_{(w)}$  can be calculated according to double-K fracture criterion and concrete fracture toughness calculation equations formulated by DL/T 5332-2005 “Norm for fracture test of hydraulic concrete” [23].

##### 3.1.1. Calculation of critical effective fracture length $a_c$

Due to stable crack extension phase of concrete specimens before unstable fracture, the actual crack length is greater than the initial crack length before unstable fracture. It is difficult to accurately measure critical crack subcritical extension length  $\Delta a_c$  and load when the crack starts to expand (crack initiation load, corresponding to  $K_{IC}^Q$ ). They are usually obtained with advanced testing technologies such as photoelastic patch. Therefore, they are more frequently got through calculation.

For the standard three-point bending beam (span-height ratio  $S/h = 3$ , hereinafter the same), the load  $P$  and CMOD has following relationship [24]:

$$\begin{cases} CMOD = \frac{6PSa}{thE} F_1(\alpha) \\ F_1(\alpha) = 0.76 - 2.28\alpha + 3.87\alpha^2 - 2.04\alpha^3 - \frac{0.66}{(1-\alpha)^2} \end{cases} \quad (1)$$

where  $P$  is load, N;  $S$  is the test piece beam span, m;  $t$  and  $h$  are the specimen width and height, m;  $a$  is the effective fracture length, m; CMOD is the crack mouth opening displacement corresponding to  $P$ , m;  $\alpha$  is the effective fracture length and specimen height ratio,  $a/h$  and  $E$  is the concrete calculation elastic modulus, MPa.

Wherein the elastic modulus  $E$  is calculated according to formula (2):

$$E = \frac{1}{tC_i} \left[ 3.70 + 32.6 \tan^2 \left( \frac{\pi a_0 + h_0}{2 h + h_0} \right) \right] \quad (2)$$

Where  $a_0$  is the initial crack degree, m;  $h_0$  is the steel sheet thickness equipped on the clip-on extensometer, m;  $C_i = V_i/F_i$  is an initial value of the specimen,  $\mu\text{m}/\text{kN}$ , which is calculated with  $V, P$  values of any point of straight line segments on curve rise.

Substitute  $P_{\max}$  and  $CMOD_C$  into formula (1) and get the nonlinear equation of  $a_c$ . Through iteration,  $a_c$  can be calculated, but the procedure is cumbersome. Literature [24] provides a simplified formula as follows:

$$CMOD = \frac{P}{Et} \left[ 3.70 + 32.60 \text{tg}^2 \left( \frac{\pi}{2} \alpha \right) \right] \quad (3)$$

Where the symbols have the same meaning as in Eqs. (1) and (2).

Calculations show that when  $0.2 \leq \alpha \leq 0.75$ , the maximum relative error between formula (3) and formula (1) is 2%. Therefore,  $a_c$  can be calculated according to formula (3):

$$a_c = \frac{\pi}{2} \text{harctg} \sqrt{\frac{Et}{32.6P} CMOD_C - 0.1135} - h_0 \quad (4)$$

### 3.1.2. Calculation of stress intensity factor $K_{IC}^C$ caused by closure stress

Because of the cracks stable expansion phase before concrete unstable fracture, according to the fictitious crack model, when the crack opening displacement  $w$  is smaller than  $w_0$  ( $w_0$  is the opening displacement when cracks cannot transfer stress), it can still pass the stress  $\sigma(w)$ , which is called closure stress. Therefore, in addition to external loads, there also exists the closure stress preventing crack propagation in three-point bending beam. Stress intensity factor caused by closure stress  $\sigma_{(w)}$  at the crack tip is denoted as  $K_{IC}^C$ . Shilang X et al. derived standard three-point bending beam specimen  $K_{IC}^C$  calculation formula based on fictitious crack model [25]:

$$K_{IC}^C = \int_{a_0}^a \frac{2}{\sqrt{\pi a}} \sigma(u) F(u, v) dx \quad (a \leq a_c) \quad (5)$$

$$F(u, v) = \frac{3.52(1-u)}{(1-u)^{3/2}} - \frac{4.35 - 5.28u}{(1-v)^{3/2}} + \left[ \frac{1.30 - 0.30u^{3/2}}{(1-u^2)^{1/2}} + 0.83 - 1.76u \right] [1 - (1-u)v]$$

$$\frac{\sigma(u)}{f_t} = \beta + (1 - \beta) \frac{u - \frac{v_0}{v}}{1 - \frac{v_0}{v}}$$

$$\beta = \frac{\sigma_s(CTOD_c)}{f_t} \quad CTOD_c = CMOD_c \{ (1 - \beta)^2 + (1.081 - 1.149\alpha)(\beta - \beta^2) \}^{1/2}$$

$$\sigma_s(CTOD_c) = f_t \left[ 1 + \left( C_1 \frac{CTOD_c}{w_0} \right)^3 \right] \exp \left( -C_2 \frac{CTOD_c}{w_0} \right) - \frac{CTOD_c}{w_0} (1 + C_1^3) \exp(-C_2)$$

In the formula,  $u = x/a$ ;  $v = a/h$ ;  $a$  is the effective fracture length, m;  $x$  is the distance from integral point to initial crack tip, m;  $f_t$  is concrete tensile strength, MPa, generally take  $f_t = 0.95 f_{sp}$  [26];  $\beta = a_0/a_c$ ;  $CTOD_c$  is the crack tip critical level opening displacement, m;  $C_1$  and  $C_2$  are concrete material constant; and  $w_0$  is the crack opening displacement when transfer stress is zero, mm, and is relevant with concrete characteristics such as strength.

Since the integral nonlinearity and integral singularity when  $u = 1$ , the above  $K_{IC}^C$  calculation process becomes very complicated. Literature [27] simplified it as follows: make  $F(u, v) = A \cdot u + B + 1/\sqrt{1-u^2}$ , then the simplified  $K_{IC}^C$  calculation method is given as follows:

$$K_{IC}^C = 2\sqrt{\frac{a}{\pi}} \times \left[ \frac{A \cdot D}{3} u^3 + \frac{A \cdot F + C \cdot D}{2} u^2 + C \cdot F \cdot u - D\sqrt{1-u^2} + F \cdot \arcsin(u) \right]_{\frac{v_0}{v}}^1 \quad (6)$$

Where  $v_0 = a_0/h$ ;  $A = \frac{2.23v^2 + 1.16v + 0.17}{(1-v)^{1.5}}$ ;  $C = \frac{1.65v^2 + 1.67v + 0.24}{(1-v)^{1.5}}$ ;  $D = \frac{f_t - \sigma_s}{v - v_0}$ ;  $F = \frac{v\sigma_s - v_0f_t}{v - v_0}$  and the other symbols are the same as defined above.

Paper [28] points out that when  $CTOD = CTOD_c$ ,  $C_1$ ,  $C_2$  and  $w_0$  values have little effect on  $K_{IC}^C$ , and  $C_1 = 3$ ,  $C_2 = 7$  and  $w_0 = 0.16$  mm are generally preferable for concrete. Qijin Zhang also calculated  $C_1 = 3$ ,  $C_2 = 7$  and  $w_0 = 0.16$  mm;  $C_1 = 2$ ,  $C_2 = 6$  and  $w_0 = 0.14$  mm; and  $C_1 = 4$ ,  $C_2 = 8$  and  $w_0 = 0.18$  mm through experiments, to verify the impact degree of changing these three parameters on  $K_{IC}^C$ . Results show that, using different  $C_1$ ,  $C_2$  and  $w_0$ , the calculated  $K_{IC}^C$  was close to each other [29]. Therefore, this paper directly takes  $C_1 = 3$ ,  $C_2 = 7$  and  $w_0 = 0.16$  mm.

### 3.1.3. Calculation of initiation toughness $K_{IC}^Q$ and unstable fracture toughness $K_{IC}^S$

The formula in [25] derived computational formula of  $K_{IC}^S$  with the boundary collocation method: for the standard three-point bending beam specimen,  $K_{IC}^S$  can be calculated as follows:

$$K_{IC}^S = \frac{1.5P_{\max}S}{th^2} \sqrt{a_c} F_1(\alpha) \quad (7)$$

$$F_1(\alpha) = \frac{1.99 - \alpha(1 - \alpha)(2.15 - 3.93\alpha + 2.7\alpha^2)}{(1 + 2\alpha)(1 - \alpha)^{3/2}}$$

$$P_{\max} = F_{\max} + \frac{mg}{2} \times 10^{-2}$$

Where  $P_{\max}$  is the ultimate load, kN;  $F_{\max}$  is the maximum load, KN;  $m$  is the mass between specimen seats, kg;  $g$  is the acceleration of gravity, 9.81 m/s<sup>2</sup>;  $S$  is the beam span, m; and  $\alpha$  is the critical effective fracture length and specimen height ratio,  $a_c/h$ .

Thus, the following is obtained:

$$K_{IC}^Q = K_{IC}^S - K_{IC}^C \quad (8)$$

Thus, according to Eq. (7), concrete  $K_{IC}^S$  can be calculated;  $K_{IC}^C$  is calculated according to formula (6); and then  $K_{IC}^Q$  is obtained according to Eq. (8).

In addition, DL/T 5332-2005 "Norm for fracture test of hydraulic concrete" also gives  $K_{IC}^Q$  calculation formula similar to formula (7). Only when calculating  $K_{IC}^Q$ ,  $a$  is taken as  $a_0$ ,  $F$  is for the crack initiation load  $F_Q$ ,  $\alpha$  is the initial crack length and specimen height ratio  $a_0/h$ , namely

$$K_{IC}^Q = \frac{1.5 \left( F_Q + \frac{mg}{2} \times 10^{-2} \right) S}{th^2} \sqrt{a_0} F_1(\alpha) \quad (9)$$

$$F_1(\alpha) = \frac{1.99 - \alpha(1 - \alpha)(2.15 - 3.93\alpha + 2.7\alpha^2)}{(1 + 2\alpha)(1 - \alpha)^{3/2}}$$

In the formula, initiation load  $F_Q$  transforms into corresponding load of elected segment turning point. A large number of experiments show that most of the turning point is in the range of  $(0.6 \sim 0.9)F_{\max}$ .

### 3.2. RSM model analysis

Most structures in cold regions of northern China are under the impact of low temperature and freeze-thaw action, resulting in freeze-thaw damage. Freezing and thawing have a

significant impact on the safety and durability of concrete structures in cold regions. There are lots of researches about effect of freeze-thaw cycles on Portland cement, but study on ASC performance degradation under freezing and thawing is still insufficient. In this study, the development law of ASC fracture properties under freezing and thawing is studied. According to ASC fracture parameters before and after freeze-thaw cycles: double- $K$  fracture toughness  $K_{IC}^Q$  and  $K_{IC}^S$ , CMOD and effective fracture length test, sol ratio, slag content and age are selected as parameters, and  $K_{IC}^Q$ ,  $K_{IC}^S$ , CMOD<sub>c</sub> and  $a_c$  are response values. Using RSM and BBD methods, influence law and degree of parameters and their interaction on ASC fracture parameters before and after freeze-thaw cycles are investigated. With Design-Expert 7.0 statistical analysis software, the regression equation prediction model is obtained, and response surface is analyzed, whose effects on ASC fracture properties are obtained.

With many specimens, the test duration time is long. In order to ensure the relationship between material strength and fracture toughness, concrete strength measurement is carried out with fracture tests.

### 3.2.1. RSM principles and advantages

In examining the impact of multivariate on concrete performance, other factors are usually fixed, while changing a single factor. Although certain effect could be received, the test amount is large and it is unable to investigate the interaction among various factors. RSM was proposed by Box and Wilson [30] in 1951, which is a combination of mathematical and statistical methods, which obtains certain data with reasonable experimental design and tests. The functional relationship between factor and response value is fitted using multiple quadratic regression equation, and the optimal process parameters are found through regression analysis, so RSM is a statistical method for solving multivariate problems.

This method is mainly used to analyze the response of interest affected by a number of variables through modeling and analysis, which can combine random and deterministic simulation problems together more easily. In this way, influence of each variable on indicators (response) in the experiment will be reflected, and the impact of interactions between variables can also be reflected, whose inner relationship is revealed with a perspective view. The ultimate aim is to optimize the response, becoming suitable for solving issues related to nonlinear data processing.

As a new experimental optimization and data processing method, RSM includes experimental design, modeling, model suitability testing, finding the best combination of conditions, and many other testing and statistical techniques that can be very suitable for experimental design and response surface analysis on experimental results.

Through process regression and response surface, contour line drawing, the response corresponding to each factor level can be easily obtained. Based on the response value of each factor level, the predicted optimal response value and corresponding experimental condition can be found, thus obtaining experimental optimal conditions ultimately.

Compared with traditional mathematical statistical methods (linear regression analysis and orthogonal design), RSM has a clear advantage in comparison. Although regression equation between the factors and response value can be obtained with experimental data through linear regression analysis, a large amount of data is required, costing much time and effort. It discusses the impact of only one factor and cannot consider the combined effect of several factors; orthogonal design focuses on scientific and reasonable arrangement for the test; and several factors may be considered at the same time and the best combination of factor levels can be found. But only isolated experimental points can be analyzed for orthogonal design, then preferred combination can only be selected from preset several experimental levels. As a result, a clear function expression, namely the regression equation between the factor and response value, cannot be given on the entire region.

The optimal condition obtained is not in the true sense, which can only be the ideal condition, so the optimal factor combination and response value cannot be given on the entire region. The RSM can consider a number of factors that affect the product at different levels; using experimental data, optimal combination problem affected by many factors can be solved through mathematical model, which is more effective than single factor analysis. Since rational experimental design is adopted, taking into account test random error, a comprehensive study on experiments with little time and small number of experiments can be conducted.

During optimization of experimental conditions, each level of experiment can be analyzed continuously. If processing response surface analysis on the experimental data is obtained, the forecasting model will generally be a curved surface, that the forecasting model is obtained continuously and then the best combination of each factor and optimal response on the entire area can be obtained.

Meanwhile, RSM fits unknown complex function on a small area with a linear or quadratic polynomial model, which has relatively simple calculation, and the obtained regression equation has higher precision.

### *3.2.2. Optimization content and procedure*

RSM optimization is usually divided into three parts:

1. **Experimental design:** there are many experimental design methods for response surface analysis, the most commonly used are Central Composite Design (CCD), Box-Behnken Design (BBD) and Plackett-Burman Design (PBD); experimental design factors may be encoded or not coded.
2. **Analysis:** complete corresponding statistical analysis such as nonlinear data fitting variance analysis, to obtain the corresponding surface equation, and evaluate the fitting result and effectiveness.
3. **Optimization:** in this module, optimization requirements can be set up, such as the highest value, lowest value or others; the software automatically calculates the optimal experiment value, and provides one or more experimental conditions under optimal results.

Specific steps of RSM optimization are as follows:

1. Determine the factors: determine the key factors to examine the process, namely important factors affecting the results within the research scope.
2. Determine the factor level: through single factor tests or determining factor level range by single factor tests or sample characteristics and process. If the scope of these levels is too wide to give precise optimum conditions, RSM with smaller factor level range can be done for more precise optimal conditions and regression equation.
3. Determine the experimental point: using appropriate experimental design to determine the experiment points. Experimental design emphasizes that test point should minimize the total experiment times. After test points are determined, experiments are carried out on the points according to the random principle. Certain data are obtained to do statistical analysis.
4. Data analysis: using appropriate statistical methods and computer program, experimental data are analyzed. Nonlinear fitting method is mainly used in response surface analysis to obtain a regression equation. The most common fitting method is the polynomial method; linear polynomial can be used in a simple relationship; quadratic polynomial can be used in a relationship containing interaction; and cubic or higher-degree polynomial can be used in more complicated interaction. A quadratic polynomial is used in general.

According to the fitting equation obtained, a response surface plot can be used to obtain the optimum value; equation solving method can also be used to obtain the optimum value. In addition, using some of the data processing software, the optimal results can be easily obtained. Statistical analysis softwares often used are SAS, SPSS and Design-Expert.

The optimization result obtained from response surface analysis is a prediction, which needs to be verified through experiments. If the corresponding prediction and experimental results are consistent according to predicted experimental conditions, then the response surface optimization analysis is successful; otherwise, it is needed to change the response surface equation, or reselect reasonable experimental factors and levels.

### 3.2.3. Data processing software Design-Expert

As the world's top-level experimental design software, Design-Expert is the easiest to use and most complete with best affinity. In RSM optimization test papers already published, Design-Expert is the most widely used software. Design-Expert software is a handy business software for response surface optimization, and it is very convenient to use in experimental design and data processing. Although not as powerful as SAS, Design-Expert can be easily used in CCD or BBD response surface analysis, the quadratic polynomial surface analysis can be accessed very well and the data processing requirements can be satisfied. Some of the operations are more convenient than SAS, and the three-dimensional effect is more intuitive. The optimization results analyzed with RSM can be automatically obtained by the software, without solving surface equation with mathematical tools like MATLAB.

During process of using the software, in order to access the experimental condition predictive value with relative accurate optimal results, the decimal digits of factor level can be set as two or more. Of course, the number of effective digits under actual experimental conditions should also be taken into account in setting the effective number of bits.

With the improvement of computer performance, RSM has become an optimization technique with high-precision, wide application and practical value. It is mainly used in three aspects [31, 32]: (1) describing the impact of a single test variable on response values; (2) determining the relationship between variables; and (3) describing the combined effects of all variables on response value.

Thus, RSM can be used in agriculture, biotechnology, food, chemistry, manufacturing and other fields, which has already been widely used in the optimization design, reliability analysis and calculation, kinetics, engineering process control and other aspects. RSM has become an effective way to reduce development costs, optimize processing conditions, improve product quality and solve practical problems in production process. But it has been rarely applied in civil engineering, even less in concrete. Therefore, this section briefly describes the RSM application principles, advantages and steps, hoping to help more researchers use RSM technology, for convenient and effective solution in the design and data processing problems, especially hoping to make RSM more widely used in concrete engineering.

Factor	Code	Levels of code		
		-1	0	1
A/S	A	0.54	0.56	0.58
Slag content/(g/cm <sup>3</sup> )	B	0.40	0.42	0.44
Age/days	C	28	60	92

**Table 3.** Levels of factors of RSM.

Test number	Design of tests			Test results			
	A	B/(g/cm <sup>3</sup> )	C/d	$K_{IC}^Q$ /MPa·m <sup>1/2</sup>	$K_{IC}^S$ /MPa·m <sup>1/2</sup>	CMOD <sub>c</sub> /mm	aC/mm
1	-1	-1	0	7.723353	11.93899	0.1257	68.3752
2	1	-1	0	4.322432	7.597456	0.1213	65.7866
3	1	0	-1	4.288812	7.586042	0.1212	65.7278
4	0	0	0	4.235751	7.546166	0.1207	65.4336
5	1	0	1	4.253227	8.028535	0.1152	62.1978
6	0	0	0	4.431611	8.196176	0.1162	62.7861
7	0	0	0	8.249791	12.45929	0.1293	69.9074
8	0	1	-1	4.199010	7.977579	0.1149	62.0213
9	-1	0	1	8.224674	12.43252	0.1291	69.8436

Test number	Design of tests			Test results			
	A	B/(g/cm <sup>3</sup> )	C/d	$K_{IC}^Q$ /MPa·m <sup>1/2</sup>	$K_{IC}^S$ /MPa·m <sup>1/2</sup>	CMOD <sub>c</sub> /mm	aC/mm
10	0	-1	1	4.183162	7.963782	0.1148	61.9624
11	1	1	0	4.026418	7.890307	0.1132	61.0211
12	-1	0	-1	4.322866	8.093164	0.1156	62.4331
13	0	-1	-1	4.117233	7.934421	0.1141	61.5506
14	-1	1	0	4.055794	7.406423	0.1191	64.4922
15	0	0	0	7.824996	12.02145	0.1286	69.0125
16	0	1	1	4.237481	8.011488	0.1149	62.1389
17	0	0	0	4.628621	8.382064	0.1173	63.4332

**Table 4.** BBD test design and the results.

### 3.2.4. Verification of RSM model

Setting  $K_{IC}^S$  as response, using Design-Expert software, BBD test data are used for quadratic regression according to **Tables 3 and 4**. Based on initial fitting equation, insignificant items are manually removed for optimization. Lack of fit of the model is ultimately determined as 0.84, the SNR value Adeq Precision is also high (142.350), showing that this model can be used to predict;  $PredR^2$  (0.9983) and  $AdjR^2$  value (0.9993) difference is very small, indicating a high degree of the response surface equation optimization, which fits well. The regression model is as shown in Eq. (10):

$$K_{IC}^S = 8.02 + 0.18A + 0.085B + 2.34C + 0.035AB + 0.082AC + 0.093BC + 0.067B^2 + 1.82C^2 \quad (10)$$

Variance analysis is done to the model and significance test is done to the regression coefficients, as shown in **Tables 5 and 6**.

	Quadratic sum	Freedom	Mean square	F value	P value
Model	58.24	8	7.28	3067.88	<0.0001
Residual error	0.019	8	2.373E-003		
Lack of fit	8.653E-003	4	2.163E-003	0.84	0.5669
Pure error	0.010	4	2.582E-003		
Sum	58.25	16			

**Table 5.** Variance analysis of the model.

	Regression coefficient	Standard deviation	Lower confidence limit of 95%	Upper confidence limit of 95%	P value
A	0.18	0.017	0.14	0.22	<0.0001
B	0.085	0.017	0.045	0.12	0.0011
C	2.34	0.017	2.30	2.38	<0.0001
AB	0.035	0.024	-0.021	0.092	0.1837
AC	0.082	0.024	0.026	0.14	0.0096
BC	0.093	0.024	0.037	0.15	0.0052
B <sup>2</sup>	0.067	0.024	0.012	0.12	0.0223
C <sup>2</sup>	1.82	0.024	1.76	1.87	<0.0001

**Table 6.** Significance test of the regression coefficients.

#### 4. Influences of freeze-thaw on $K_{IC}^S$ under different slag content

Influence of freeze-thaw on  $K_{IC}^S$  under different slag content is shown in **Figure 3**.

Various factors may result in the material deterioration and failure of concrete as described above, and the seriousness caused depends to a great extent on the porosity and permeability of internal texture of concrete itself [33, 34]. Generally, if the compactness of a concrete structure is poor or its internal porosity is considerable, more possibly various liquids and gases penetrate into its interior with more quantity and larger depth, than the carbonation layer, and chemical corrosion of concrete and the rust of reinforcement is accelerated, even the liquid can pass easily through the structure.

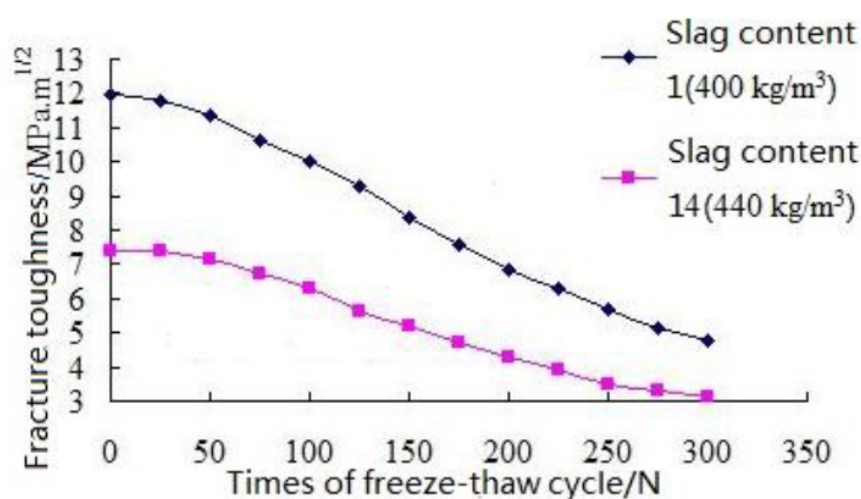


**Figure 3.** Influence of freeze-thaw on  $K_{IC}^S$  under different slag content.

The main factors having influence on texture and porosity of concrete are water-cement ratio (or water-binder ratio); kind and fineness of cement; kind of aggregate; producing quality and curing condition. Producing quality and curing condition can be paid attention during construction, but the first three factors are mainly influenced by material characteristic itself.

ASC has a compact structure, which is able to well resist penetration of water and air. Since the strength enhancement of ASC tends to grow at a relatively slow speed, when it is exposed to freeze-thaw cycles, ASC could continue to form hardened structure, which is beyond the destroying speed. Therefore, ASC could be a desirable material to resist carbonation as well as freeze-thaw attack in concrete structures.

## 5. Conclusions

1. The calculation procedure of ASC fracture parameters is studied. With the CMOD, other indexes including concrete effective fracture length; CTOD; and stress intensity factors  $K_{IC}^C$ ,  $K_{IC}^Q$  and  $K_{IC}^S$  from closure stress  $\sigma(w)$  can be calculated. And critical effective fracture length  $a_C$ , stress intensity factor  $K_{IC}^C$  caused by closure stress, initiation toughness  $K_{IC}^Q$  and unstable fracture toughness  $K_{IC}^S$  are analyzed specifically.
2. The RSM theory is systematically investigated. RSM principles and advantages, optimization content and procedure, data processing software Design-Expert and verification of RSM model are provided. Results show that RSM is suitable for ASC fracture property analysis.
3. Influences of freeze-thaw on  $K_{IC}^S$  under different slag content are put forward. The main reason for good freezing resistance is that ASC has a dense structure, which is beneficial for preventing water and air penetration. Such property indicates that ASC could have good performance in carbonation environment.
4. In this study, through calculation and analysis, the calculation approach of fracture parameters is researched; theoretical study of RSM is summarized; and the reason why ASC performs well under freeze-thaw cycles is studied. However, since ASC fracture properties are influenced by various factors, more research should be carried out. What is more, the RSM theory is seldom used in ASC analysis, it is worth more deeper and systematical investigation. The ASC performances also require more focus from the angle of cross-disciplinary methods including materials science, mechanics and structural analysis.

## Acknowledgements

The author wishes to express his gratitude and sincere appreciation to the National Natural Science Fund [Grant Number: 51578540] for financing this research work and several ongoing research projects related to the properties of ASC.

## Author details

Qixuan Li

Address all correspondence to: liqixuan19921210@163.com

Air Force Engineering University, Xi'an, China

## References

- [1] Sun W, Zhang YM, Yan HD, Mu R. Damage and damage resistance of high strength concrete under the action of load and freeze-thaw cycles. *Cem Concr Res* 1999; 29(9): 1519–1523. doi:10.1016/S0008-8846(99)00097-6.
- [2] Shojaei M, Behfarnia K, Mohebi R. Application of alkali-activated slag concrete in railway sleepers. *Mater Des* 2015; 69: 89–95. doi:10.1016/j.matdes.2014.12.051.
- [3] Ren WB, Xu JY, Bai EL. Strength and ultrasonic characteristics of alkali-activated fly ash-slag geopolymer concrete after exposure to elevated temperatures. *J Mater Civ Eng* 2016; 28(2). doi:10.1061/(ASCE)MT.1943-5533.0001406.
- [4] Mithun BM, Narasimhan MC. Performance of alkali activated slag concrete mixes incorporating copper slag as fine aggregate. *J Clean Prod* 2016; 112: 837–844. doi:10.1016/j.jclepro.2015.06.026.
- [5] Gao Y, Xu JY, Bai EL, Luo X, Zhu JS, Nie LX. Static and dynamic mechanical properties of high early strength alkali activated slag concrete. *Ceram Int* 2015; 41(10): 12901–12909. doi:10.1016/j.ceramint.2015.06.131.
- [6] Okoye FN, Durgaprasad J, Singh NB. Mechanical properties of alkali activated flyash/ Kaolin based geopolymer concrete. *Constr Build Mater* 2015; 98: 685–691. doi:10.1016/j.conbuildmat.2015.08.009.
- [7] Torres-Carrasco M, Tognonvi MT, Tagnit-Hamou A, Puertas F. Durability of alkali-activated slag concretes prepared using waste glass as alternative activator. *ACI Mater J* 2015; 112(6): 791–800.

- [8] Kim SW, Jang SJ, Kang DH, Ahn KL, Yun HD. Mechanical properties and eco-efficiency of steel fiber reinforced alkali-activated slag concrete. *Mater* 2015; 8(11): 7309–7321. doi: 10.3390/ma8115383.
- [9] Krivenko P, Kovalchuk G. Achieving a heat resistance of cellular concrete based on alkali activated fly ash cements. *Mater Struct* 2015; 48(3): 599–606. doi:10.1617/s11527-014-0479-0.
- [10] Ravikumar D, Neithalath N. Electrically induced chloride ion transport in alkali activated slag concretes and the influence of microstructure. *Cem Concr Res* 2013; 47: 31–42. doi:10.1016/j.cemconres.2013.01.007.
- [11] Ravikumar D, Neithalath N. An electrical impedance investigation into the chloride ion transport resistance of alkali silicate powder activated slag concretes. *Cem Concr Compos* 2013; 44: 58–68. doi:10.1016/j.cemconcomp.2013.06.002.
- [12] Qixuan Li, LiangcaiCai, Yawei Fu, Haifu Wang, Yong Zou. Fracture properties and response surface methodology model of alkali-slag concrete under freeze-thaw cycles. *Constr Build Mater* 2015; 93: 620–626. doi:10.1016/j.conbuildmat.2015.06.037.
- [13] Provis JL, Palomo A, Shi CJ. Advances in understanding alkali-activated materials. *Cem Concr Res* 2015; 78: 110–125. doi:10.1016/j.cemconres.2015.04.013.
- [14] Kovtun M, Kearsley EP, Shekhovtsova J. Chemical acceleration of a neutral granulated blast-furnace slag activated by sodium carbonate. *Cem Concr Res* 2015; 72: 1–9. doi: 10.1016/j.cemconres.2015.02.014.
- [15] Ma Y, Ye G. The shrinkage of alkali activated fly ash. *Cem Concr Res* 2015; 68: 75–82. doi:10.1016/j.cemconres.2014.10.024.
- [16] Ke XY, Bernal SA, Provis JL. Controlling the reaction kinetics of sodium carbonate-activated slag cements using calcined layered double hydroxides. *Cem Concr Res* 2016; 81: 24–37. doi:10.1016/j.cemconres.2015.11.012.
- [17] GB/T 18046-2000. Ground granulated blast furnace slag used for cement and concrete. Beijing: The state bureau of quality and technical; 2000.
- [18] GB/T 18736-2002. Mineral admixtures for high strength and high performance concrete. Beijing: General Administration of Quality Supervision, Inspection and Quarantine of the People's Republic of China; 2002.
- [19] GB/T 12957/2005. Test method for activity of industrial waste slag used as addition to cement. Beijing: General Administration of Quality Supervision, Inspection and Quarantine of the People's Republic of China; 2005.
- [20] GB/T 50080-2002. Standard for test method of performance on ordinary fresh concrete. Beijing: Ministry of Construction of the People's Republic of China; 2003.
- [21] GB/T 50081-2002. Standard for test method of mechanical properties on ordinary concrete. Beijing: Ministry of Construction of the People's Republic of China; 2003.

- [22] Thomas RJ, Peethamparan S. Alkali-activated concrete: engineering properties and stress-strain behavior. *Constr Build Mater* 2015; 93: 49–56. doi:10.1016/j.conbuildmat.2015.04.039.
- [23] DL/T 5332-2005. Norm for fracture test of hydraulic concrete. Beijing: National Development and Reform Commission; 2005.
- [24] Tada H, Paris PC, Irwin GR. The stress analysis of cracks handbook. St. Louis: Parris Productions Incorporated; 1985.
- [25] Shilang X, Reinhardt HW. A simplified method for determining double-K fracture parameters for three-point tests. *Int J Fract* 2000; 10(4): 181–209. doi:10.1023/A:1007676716549.
- [26] Swaddiwudhi Pong S, Lu HR, Wee TH. Direct tension test and tensile strain capacity of concrete at early age. *Cem Concr Res* 2003; 33: 2077–2084. doi:10.1016/S0008-8846(03)00231-X.
- [27] Shilang X, Zhimin W, Ding S. A practical analytical approach to the determination of double-K fracture parameters of concrete. *Eng Mech* 2003; 20(3): 54–62. doi:10.3969/j.issn.1000-4750.2003.03.010.
- [28] Reinhardt HW, Comelissen HAW, Hordijk DA. Tensile tests and failure analysis of concrete. *J Struct Eng* 1986; 112(11): 2462–2477.
- [29] Zhang Q. Experimental research on high strength wear-resistant concrete cracking and fracture properties [thesis]. Hangzhou: Zhejiang University; 2008.
- [30] Box GEP, Wilson KB. On the experimental attainment of optimum conditions. *J R Stat Soc Ser B-Stat Methodol* 1951; 13(1): 1–45.
- [31] Ambati P, Ayyanna C. Optimizing medium constituents and fermentation conditions for citric acid production from palmyrajaggery using response surface method. *World J Microbiol Biotechnol* 2001; 17(4): 331–335. doi:10.1023/A:1016613322396.
- [32] Ahuja SK, Ferreira GM, Moreira AR. Application of plackett-burman design and response surface methodology to achieve exponential growth for aggregated shipworm bacterium. *Biotechnol Bioeng* 2004; 85(6): 666–675. doi:10.1002/bit.10880.
- [33] Jo BW, Park SK, Park JB. Properties of concrete made with alkali-activated fly ash lightweight aggregate (AFLA). *Cem Concr Compos* 2007; 29(2): 128–135. doi:10.1016/j.cemconcomp.2006.09.004.
- [34] Krivenko P, Drochytka R, Gelevera A, Kavalerova E. Mechanism of preventing the alkali-aggregate reaction in alkali activated cement concretes. *Cem Concr Compos* 2014; 45: 157–165. doi:10.1016/j.cemconcomp.2013.10.003.